
01 Sep 2005

The Processing, Mechanical Properties and Bioactivity of Zinc based Glass Ionomer Cements

D. Boyd

Mark R. Towler

Missouri University of Science and Technology, mtowler@mst.edu

Follow this and additional works at: https://scholarsmine.mst.edu/che_bioeng_facwork

 Part of the [Biochemical and Biomolecular Engineering Commons](#), and the [Biomedical Devices and Instrumentation Commons](#)

Recommended Citation

D. Boyd and M. R. Towler, "The Processing, Mechanical Properties and Bioactivity of Zinc based Glass Ionomer Cements," *Journal of Materials Science: Materials in Medicine*, vol. 16, no. 9, pp. 843 - 850, Springer, Sep 2005.

The definitive version is available at <https://doi.org/10.1007/s10856-005-3578-1>



This work is licensed under a [Creative Commons Attribution 4.0 License](#).

This Article - Journal is brought to you for free and open access by Scholars' Mine. It has been accepted for inclusion in Chemical and Biochemical Engineering Faculty Research & Creative Works by an authorized administrator of Scholars' Mine. This work is protected by U. S. Copyright Law. Unauthorized use including reproduction for redistribution requires the permission of the copyright holder. For more information, please contact scholarsmine@mst.edu.

The processing, mechanical properties and bioactivity of zinc based glass ionomer cements

D. BOYD, M. R. TOWLER*

Materials & Surface Science Institute, University of Limerick, Ireland

E-mail: Mark.Towler@ul.ie

The suitability of Glass Ionomer Cements (GICs) for use in orthopaedics is retarded by the presence in the glass phase of aluminium, a neurotoxin. Unfortunately, the aluminium ion plays an integral role in the setting process of a GIC and its absence is likely to hinder cement formation. However, zinc oxide, a bactericide, can act both as a network modifying oxide and an intermediate oxide in a similar fashion to alumina and so ternary systems based on zinc silicates often have extensive regions of glass formation. The purpose of this research was to produce novel GICs based on calcium zinc silicate glasses and to evaluate their rheological, mechanical and biocompatible properties with the ultimate objective of developing a new range of cements for skeletal applications. The work reported shows that GICs based on two different glasses, A and B ($0.05\text{CaO} \cdot 0.53\text{ZnO} \cdot 0.42\text{SiO}_2$ and $0.14\text{CaO} \cdot 0.29\text{ZnO} \cdot 0.57\text{SiO}_2$, respectively), exhibited handling properties and flexural strengths comparable to conventional GICs. Upon immersion in simulated body fluid of a GIC based on glass B, an amorphous calcium phosphate layer nucleated on the surface of the cement indicating that these cements are bioactive in nature.

© 2005 Springer Science + Business Media, Inc.

1. Introduction

Polymethylmethacrylate (PMMA) bone cement is currently the only material used for anchoring cemented arthroplasties to contiguous bone [1]. However, there are major concerns regarding using PMMA invasively. The methylmethacrylate monomer is known to cause necrosis of healthy bone stock and it has been implicated in acute cardiovascular and respiratory reactions during cementation [2–4]. Another drawback of PMMA is that it cannot form a direct chemical bond, only a mechanical interlock, with bone [5]. There is clearly a requirement for biocompatible adhesive bone cements for the fixation of arthroplasty components.

Glass ionomer cements (GICs) developed in the late 1960's at the Laboratory of the Government Chemist (London, UK) are now used extensively in dental applications as luting cements and as colour matched alternatives to amalgam restoratives [6]. They have potential as bone cements because of their ability to adhere to both surgical metals and the mineral phase of bone [7, 8]. They set without shrinkage [9] or significant heat evolution [10] and have mechanical properties comparable to bone. GICs chemically bond with hydroxyapatite (HA) [8, 11] as well as releasing clinically beneficial amounts of active ions, such as fluoride, which can help to prevent secondary caries [12]. GICs set by the reaction of an aluminosilicate glass with an aqueous solution of polyalkenoic acid (PAA); the acid attacks and degrades the glass structure, releasing metal cations into

the aqueous phase. These cations then become chelated by the carboxylate groups on the acid chains and serve to crosslink the matrix [6, 11]. The set cement consists of reacted and un-reacted glass particles embedded in a hydrated polysalt matrix. The setting process is a continuous process evidenced by a change in mechanical properties with time [13].

The presence of aluminium in the glass phase of all commercially available GICs has restricted their widespread use in orthopaedics, as aluminium is believed to cause defective bone mineralisation [14, 15], inhibiting the formation of a stable bond between GIC and bone. The Al^{3+} ion has also been implicated in the pathogenesis of many degenerative brain diseases including Parkinson's and Alzheimer's disease [16–19], and the release of aluminium from GIC used in reconstructive otoneurosurgery has been considered as the principle cause of one case of sub-acute fatal encephalopathy [20]. However, the aluminium ion plays an integral role in the setting process of a GIC and its absence can hinder cement formation [21]. Fortunately, zinc oxide (ZnO) can act as both a network modifying oxide and an intermediate oxide in a similar fashion to alumina [22]. This results in ternary systems based on zinc silicates (with the exception of those containing alumina) often having extensive regions of glass formation [23]. Zinc silicate glasses containing no alumina are therefore suitable for forming polyalkenoate cements. The ability of aluminium-free GICs to be

*Author to whom all correspondence should be addressed.

produced based on ZnO has already been demonstrated [24, 25]. As well as acting as a direct replacement for aluminium, zinc also has the ability to increase the DNA of osteoblasts [26], resulting in increased bone mass [27]. Therefore its inclusion in GICs for orthopaedic applications is likely to have a positive effect *in vivo*.

The development of bioactive aluminium-free GICs is of considerable interest in clinical orthopaedics. Bioactive materials can bond directly to living bone through the formation of an apatite layer [28]. In order to reproduce the formation of apatite layers on potential bioactive materials *in vitro*, Kokubo *et al.* [29] developed acellular simulated body fluid (SBF) that has inorganic ion concentrations similar to human body fluid. In a recent study by Kamitakahara *et al.* [30], the suitability of GICs for bone cementation has been questioned as the authors found that it was not possible for apatite to form on conventional GICs after immersion in SBF. The study concluded that the presence of small quantities of PAA released from the GICs inhibits apatite formation. It is the purpose of this study to examine the effect of PAA molecular weight, concentration, and maturation time on the mechanical properties of zinc-based GICs and subsequently to show that these GICs form apatite on their surface within 24 h, which is in direct disagreement with the work of Kamitakahara *et al.* [30].

2. Materials and methods

2.1. Glass synthesis

Two glass compositions were produced and are illustrated in Table I. Glass A has a minimal calcium loading and glass B corresponds to a eutectic point on the relevant ternary diagram, chosen from this system on the basis of ease of glass formation [23]. Appropriate amounts of analytical grade silica, zinc oxide and calcium carbonate were weighed out in a plastic tub and mixed in a ball mill for one hour, then dried in a vacuum oven (100 °C, 1 h). The pre-fired glass batch was then transferred to a mullite crucible for firing (1480 °C, 1 h). The glass melts were then shock quenched into demineralised water. The resulting frit was dried then ground and sieved. The glass that passed through a <45 µm sieve was used to form the cements.

2.2. Poly(acrylic) acid

Ciba speciality polymers (Bradford, UK) supplied the PAA in aqueous solution (25% m/w). These acids were coded E7 and E9. Each was freeze-dried, ground and sieved to retrieve a <90 µm powder for each acid. The molecular weights of the acids have been determined previously [31] and are presented in Table II.

TABLE I Glass compositions (mol%)

| | CaO | ZnO | SiO ₂ |
|---------|------|------|------------------|
| Glass A | 0.05 | 0.53 | 0.42 |
| Glass B | 0.14 | 0.29 | 0.57 |

TABLE II Molar mass details of the poly(acrylic) acids

| CODE | Mw | Mn | PD | Peak Mol. Wt. |
|------|--------|--------|-----|---------------|
| E7 | 25,700 | 8,140 | 3.2 | 19,100 |
| E9 | 80,800 | 26,100 | 3.1 | 83,500 |

TABLE III Cement formulations examined in this study. X denotes the use of E7 or E9 acids

| Cement formulations | Amount of glass (g) | Amount of PAA (g) | Amount of water (ml) |
|---------------------|---------------------|-------------------|----------------------|
| AX 40 wt% Series | 1 | 0.36 | 0.55 |
| AX 46 wt% Series | 1 | 0.42 | 0.495 |
| AX 50 wt% Series | 1 | 0.455 | 0.455 |
| BX 40 wt% Series | 1 | 0.195 | 0.3 |
| BX 46 wt% Series | 1 | 0.23 | 0.27 |
| BX 50 wt% Series | 1 | 0.25 | 0.25 |

2.3. Cement preparation

Cements were prepared by thoroughly mixing the glass powders (<45 µm) with the PAA and distilled water on a glass plate. Complete mixing was undertaken within 30 s. The twelve cement formulations examined are illustrated in Table III. The concentrations of the PAA solutions are expressed in percent by mass (grams of solute/grams of solution).

2.4. Determination of working and setting times

The working and setting times of the cements were measured in accordance with ISO9917E [32]. The mean setting time of 3 tests was recorded.

2.5. Preparation of compression test specimens

Compression testing was undertaken in accordance with ISO9917E [32]. Samples were tested after 1, 7, 30 and 90 days. Testing was undertaken on an Instron 4082 (Bucks, UK) using a 5 kN load cell at a crosshead speed of 1 mm min⁻¹.

2.6. Preparation of biaxial disc specimens

The flexural strength of the cements was determined by the method of Williams *et al.* [33, 34]. Samples were tested after 1, 7, 30 and 90 days. Testing was undertaken on an Instron 4082 (Bucks, UK) using a 1 kN load cell at a crosshead speed of 1 mm min⁻¹.

2.7. Testing in Simulated Body Fluid (SBF)

SBF was produced in accordance with the literature [29]. The composition is illustrated in Table IV. The ionic concentrations (mM) of SBF and human blood plasma are compared in Table V. The reagents were dissolved into 500 ml of purified water using a magnetic stirrer. The solution was maintained at 36.5 °C using a water bath. 1 N-HCl was titrated to adjust the pH of the SBF to 7.40. Purified water was then used to adjust the

TABLE IV Composition of SBF in order of addition to water

| Order | Reagent | Amount |
|-------|--|---------|
| 1 | NaCl | 7.996 g |
| 2 | NaHCO ₃ | 0.350 g |
| 3 | KCl | 0.224 g |
| 4 | K ₂ HPO ₄ ·3H ₂ O | 0.228 g |
| 5 | MgCl ₂ ·6H ₂ O | 0.305 g |
| 6 | 1N-HCl | 40 mL |
| 7 | CaCl ₂ | 0.278 g |
| 8 | Na ₂ SO ₄ | 0.071 g |
| 9 | NH ₂ C(CH ₂ OH) ₃ | 6.057 g |

TABLE V Ion concentrations (mM) of SBF and human blood plasma

| Ion | SBF | Blood plasma |
|--------------------------------|-------|--------------|
| Na ⁺ | 142.0 | 142.0 |
| K ⁺ | 5.0 | 5.0 |
| Mg ²⁺ | 1.5 | 1.5 |
| Ca ²⁺ | 2.5 | 2.5 |
| Cl ⁻ | 147.8 | 103.0 |
| HCO ₃ ⁻ | 4.2 | 27.0 |
| HPO ₄ ³⁻ | 1.0 | 1.0 |
| SO ₄ ²⁻ | 0.5 | 0.5 |

total volume of liquid to 1 litre. The SBF was stored in a refrigerator for a maximum of 3 days. Any SBF that formed precipitates during storage was discarded. The two cements with the best mechanical properties were chosen for the SBF trial. Cement discs ($n = 5$) were produced in an identical fashion to the biaxial samples and were subsequently stored in SBF for 1, 7, 30, and 90 days. A Philips Xpert MPD Pro 3040/60 X-ray Diffraction (XRD) Unit (Philips, Netherlands) was used to perform glancing angle XRD (G-XRD) at the surface of cements soaked in SBF. The incident beam was fixed at 3° relative to the sample surface. The detector (step size of 0.0083°, 10 s per step) was used to collect diffraction patterns through 0–67°.

A JOEL JSM-840 scanning electron microscope equipped with a Princeton Gamma Tech (PGT) energy Dispersive X-ray (EDX) system was used to obtain secondary electron images and carry out chemical analysis of the surface of cement discs. All EDX spectra were collected at 20 kV, using a beam current of 0.26 nA. Quantitative EDX converted the collected spectra into concentration data by using standard reference spectra obtained from pure elements under similar operating parameters. Table VI illustrates the Ca:P ratio at the surface of BE9/50 wt% discs stored in SBF stored up to 90 days.

TABLE VI Normal wt% of Ca and P at the surface of BE9 50 wt% after soaking in SBF up to 90 days

| Element | wt% at 1 day | wt% at 7 day | wt% at 30 days | wt% at 90 days |
|---------|-----------------|-----------------|-------------------|-------------------|
| Ca | 7.93 | 10.04 | 9.95 | 9.15 |
| P | 7.18 | 6.27 | 5.49 | 6.716 |
| Ca/P | 1.10 | 1.60 | 1.81 | 1.36 |

TABLE VII Working and setting times for Zn based GIC

| Cement Formulation | Working time (s) | Net setting time (s) |
|-----------------------|---------------------|-------------------------|
| AE7/40 | 72 | 390 |
| AE7/46 | 57 | 362 |
| AE7/50 | 50 | 248 |
| AE9/40 | 32 | 203 |
| AE9/46 | 28 | 168 |
| AE9/50 | 24 | 155 |
| BE7/40 | 218 | 883 |
| BE7/46 | 149 | 848 |
| BE7/50 | 122 | 832 |
| BE9/40 | 58 | 232 |
| BE9/46 | 53 | 218 |
| BE9/50 | 46 | 174 |

3. Results

3.1. Working and setting times

Table VII illustrates the working and setting times of all cement formulations with respect to ISO9917 requirements for luting cements and bases/lining cements. The results indicate all formulations except those of glass B mixed with E7 PAA are ISO compliant.

3.2. Compressive and flexural strength testing

Figs. 1 to 4 illustrate the effect of maturation time and PAA concentration and molecular weight on the compressive and flexural strengths of the GICs. The data shows that increasing PAA molecular weight, PAA concentration and aging time increase the compressive strength and flexural strength of the cements. The data also indicates that glass A produces stronger cements than glass B.

3.3. Results of SBF trial

The best performing GICs as determined by mechanical testing, AE9/50 wt% and BE9/50 wt%, were chosen for the SBF trial. Fig. 5 illustrates the effect of soaking AE9 cement in SBF. Figs. 6 and 7 illustrate the effects of soaking BE9 cement in SBF. Fig. 8 illustrates the G-XRD results for the surface of AE9 50 wt% cements soaked in SBF, and shows the formation of hopeite at the surface of the cement. Fig. 9 illustrates the G-XRD results for the surface of BE9/50 wt% cements soaked in SBF. No significant peaks were detected.

4. Discussion

4.1. Working and setting times

The results indicate that glass A is more reactive than glass B. Glass A contains only 5 mol% Ca²⁺ which can facilitate the charge balanced isomorphous replacement of SiO₄ tetrahedra in the glass structure, with ZnO₄ tetrahedra; the remaining Zn will be forced to act as a network modifier serving to increase the disruption of the glass and increase its susceptibility to acid attack. For glass B there is far more Ca²⁺ (14 mol%) acting as charge balancing cations, which allows for the stabilisation of more ZnO₄ tetrahedra in glass B making it

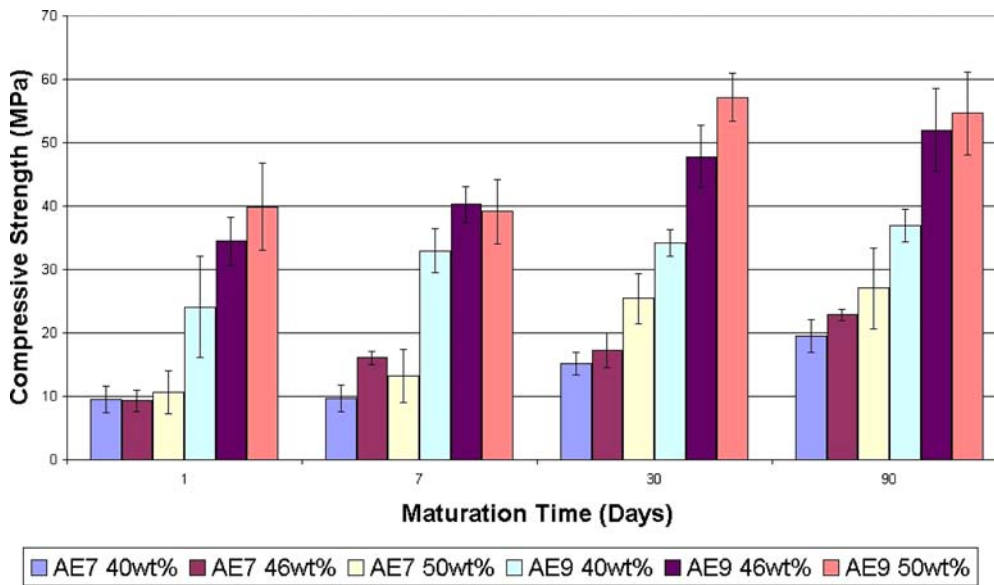


Figure 1 Change in compressive strength of cements based on glass A, with respect to PAA Mw, PAA concentration and aging time.

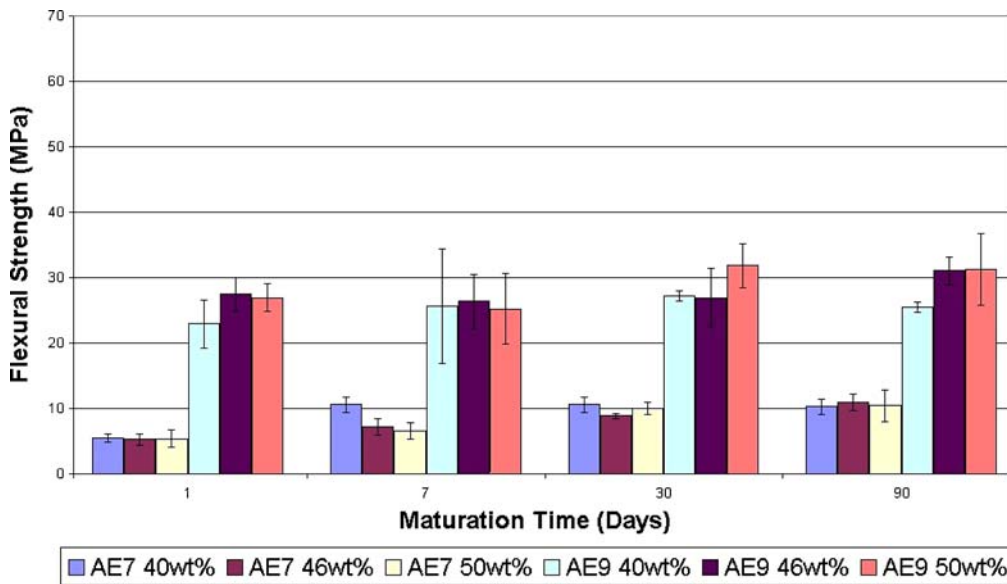


Figure 2 Change in flexural strength of cements based on glass A, with respect to PAA Mw, PAA concentration and aging time.

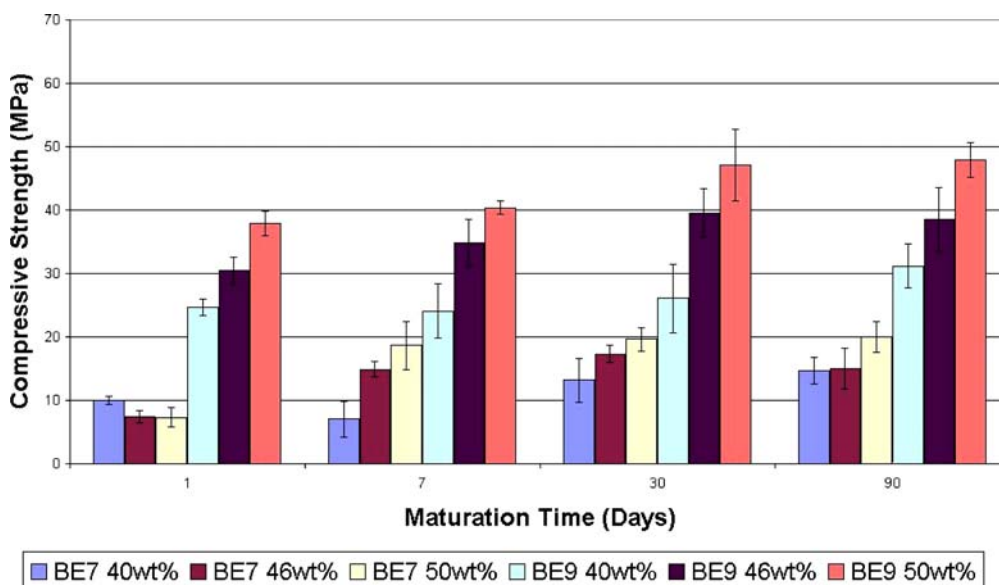


Figure 3 Change in compressive strength of cements based on glass B, with respect to PAA Mw, PAA concentration and aging time.

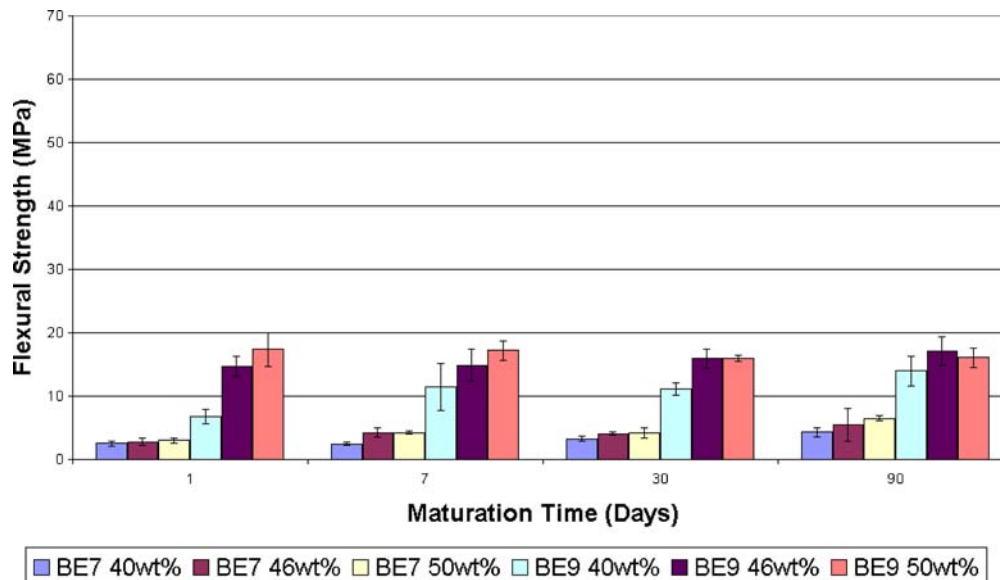


Figure 4 Change in flexural strength of cements based on glass B, with respect to PAA Mw, PAA concentration and aging time.

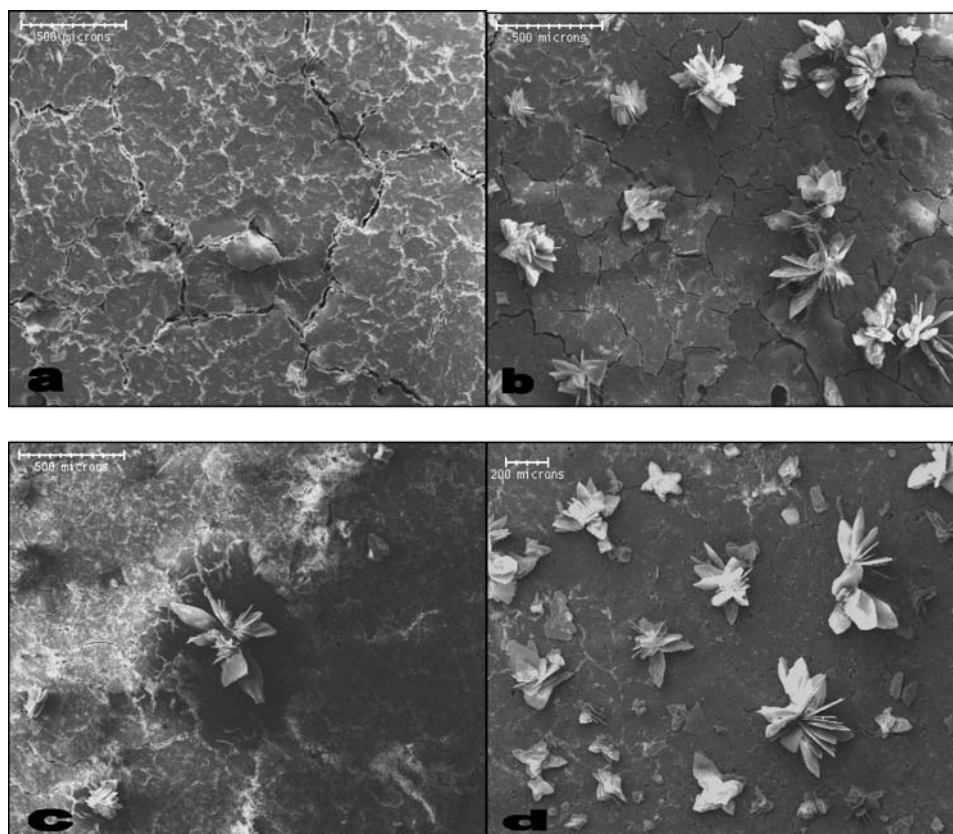


Figure 5 Illustrating the formation of hopeite on the surface of AE9/50 wt% cement, all micrographs taken at 50X magnification. (a) Shows the surface after one day soaking in SBF, a small nucleus is present after 24 h. (b) After 7 days there is widespread coverage of the surface. (c) Surface after 30 days. (d) Surface after 90 days.

less reactive than glass A. The results also indicate that as the concentration of PAA, or the molecular weight of PAA is increased the setting time decreases, following the same trends as conventional aluminium based GICs [6].

4.2. Compressive and flexural properties

The results show that GICs can be produced from reacting PAA with calcium-zinc-silicate glasses. The com-

pressive and flexural strengths of these cements increase with maturation time and both molecular weight and concentration of PAA, following the same trends as conventional aluminium-based GICs [31, 35]. Although these novel GICs exhibit strength development trends similar to conventional GICs, the compression results show that these materials are approximately one quarter the strength of their aluminium containing counterparts after 30 days maturation [35] and their compressive strength after 24 h is not sufficient

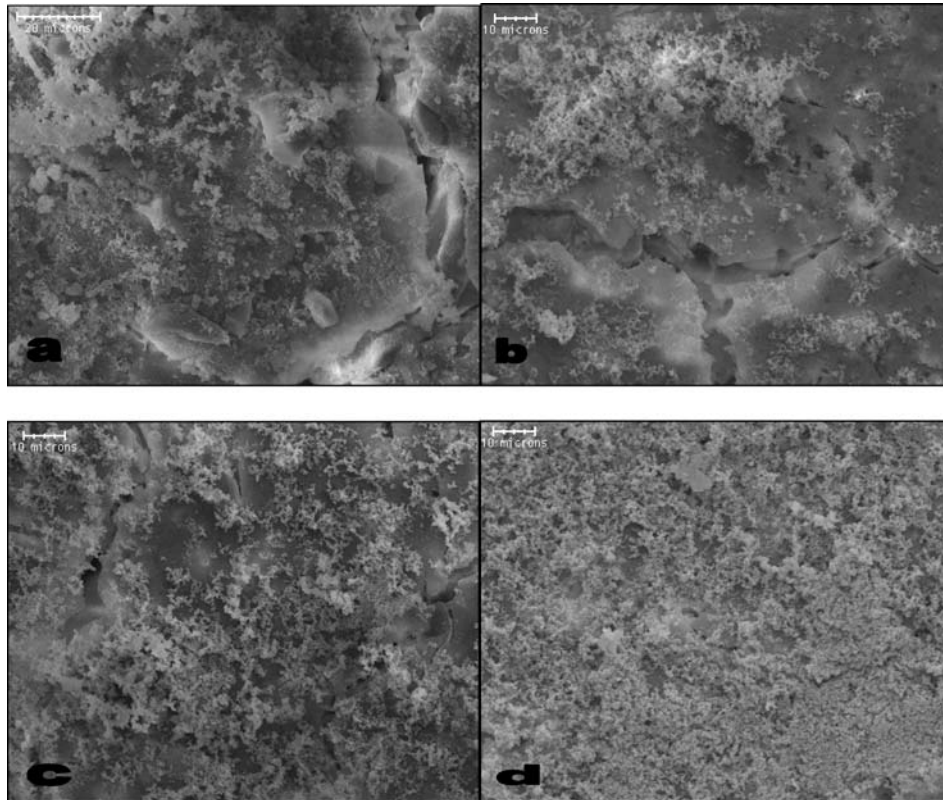


Figure 6 Illustrating the formation of ACP at the surface of BE9/50 wt% after soaking in SBF, all micrographs taken at 1000X magnification. (a) After 24 h ACP is present at the surface. (b) Clusters have become denser at 7 days. (c) After 30 days the entire sample has been covered by ACP. (d) The ACP layer has become extremely dense at the surface of the cement.

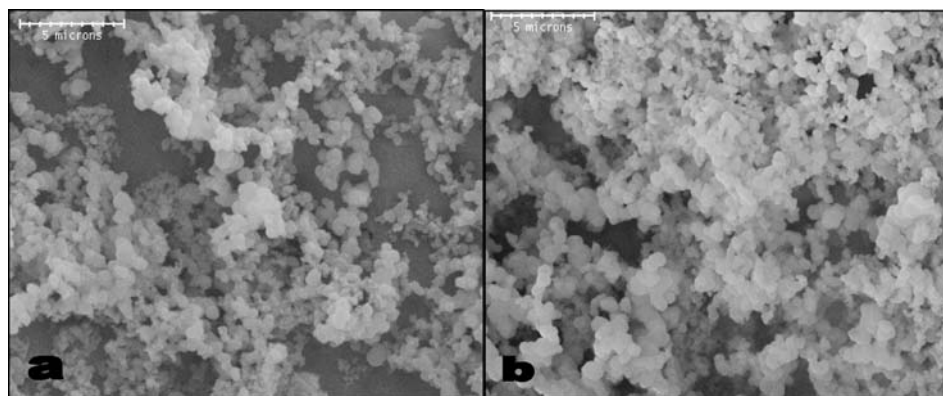


Figure 7 Illustrates the spherical nature of the ACP layer on BE9/50 wt%, images at 5000X. (a) Taken at 30 days. (b) Taken at 90 days.

to satisfy ISO9917 (70 MPa) [32]. The mean compressive strength of AE9/50 wt% cement is 57 MPa after 30 days. This is comparable to a compressive strength for Simplex P (an acrylic orthopaedic cement) of 67 MPa tested using ISO9917 criteria, and only 10 MPa short of the ISO9917 requirements [32]. ISO5833 [36] dictates flexural moulds that cannot be filled homogeneously by GIC and so the method of Williams *et al.* was chosen [33]. The flexural strengths of these cements are directly comparable to the flexural strengths of conventional GICs; the presence of labile ionic bonds between Zn^{2+} ions and the carboxylate groups on the PAA [37] facilitate such high flexural strengths. It is likely that the strengths of these cements can vastly be improved upon by encapsulation and the use of a higher molecular weight PAA, in a similar fashion to conventional GICs.

4.3. SBF trial

Fig. 5 illustrates the formation of hopeite ($Zn_3(PO_4)_2 \cdot 4H_2O$) at the surface of cement AE9/50 wt%. Insufficient levels of Ca^{2+} are leached into solution due to the low calcium content in the glass and the ionic activity product (IP) of HA cannot be raised to the required level to induce the nucleation of apatite at the cement surface. Instead, high concentrations of zinc are released and supersaturate the SBF-cement interface with respect to hopeite. This occurs in the first 24 h after immersion. Increasing numbers of hopeite crystals are apparent for each subsequent immersion time, indicating a continuous release of zinc from the set cement. Hopeite is not normally found in biological tissues, however the crystallization of zinc phosphates is not uncommon in dental materials. These crystals are loosely bound to

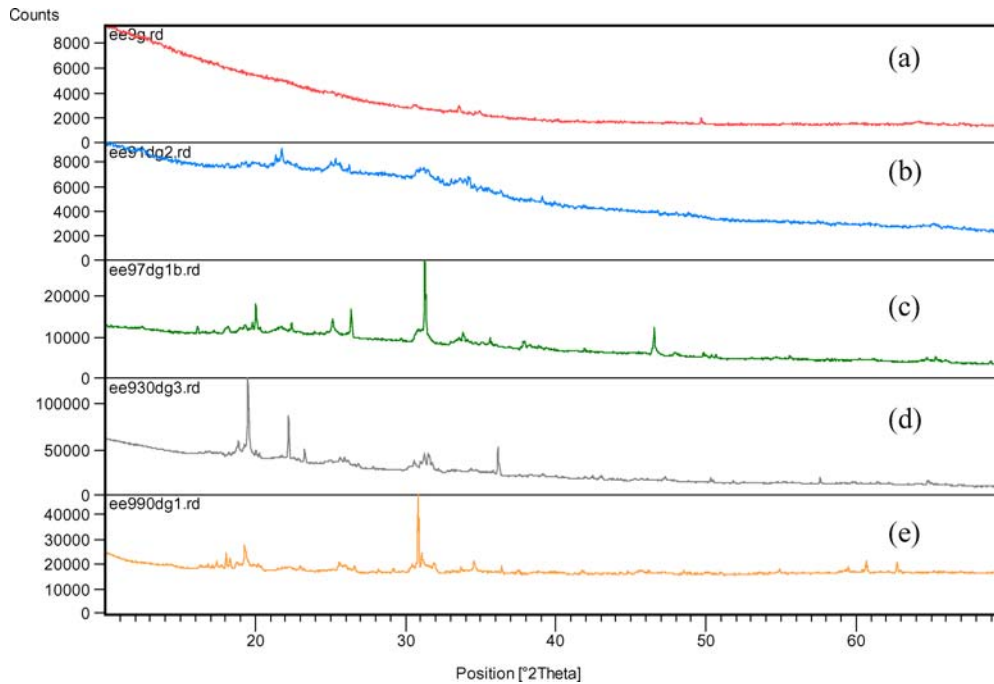


Figure 8 G-XRD on AE9/50 wt% cement soaked in SBF. (a) control sample not soaked in SBF. (b) surface after 1 day, (c) surface after 7 days, (d) surface after 30 days, (e) surface after 90 days.

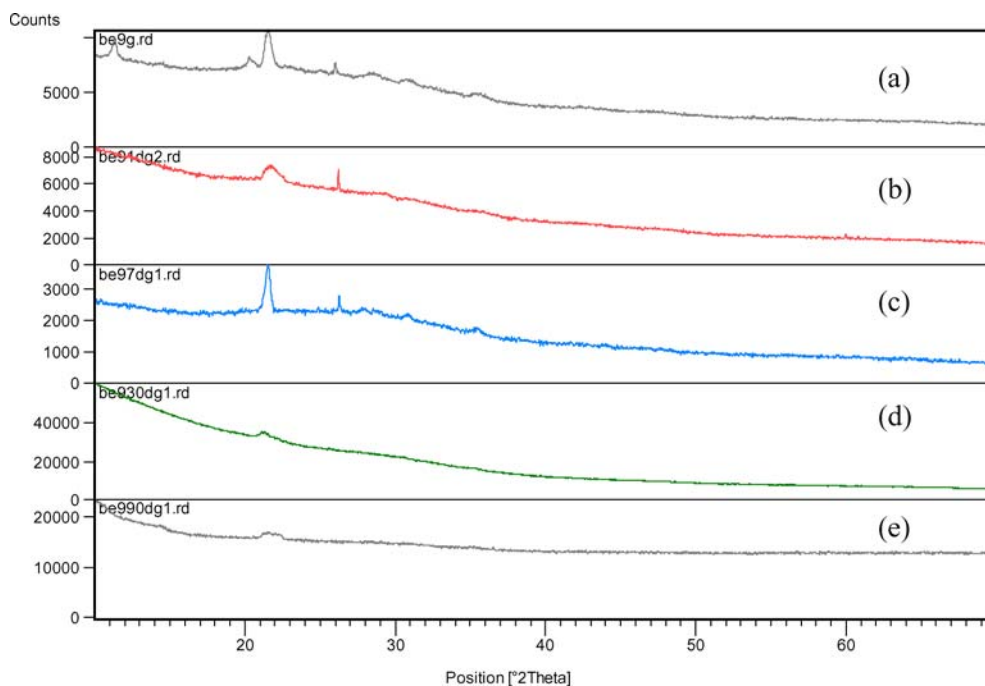


Figure 9 G-XRD on BE9/50 wt% cement soaked in SBF. (a) control sample not soaked in SBF. (b) surface after 1 day, (c) surface after 7 days, (d) surface after 30 days, original peaks in the cement become hidden by the new surface layer (e) surface after 90 days.

the surface and in zinc phosphate dental cements have been blamed for the lack of adhesion between cements and apatite [11].

Conversely, the SEM and EDX results for BE9/50 wt% indicate the presence of a calcium phosphate at the surface of the cement (Figs 6 and 7 and Table VI). In the case of this cement the glass phase contains considerably less ZnO and more CaO than AE9/50 wt%, and can therefore increase the IP of HA to a sufficient level to induce the nucleation of a calcium phosphate at the cement surface, without supersaturating the SBF with respect to hopeite. The calcium

phosphate layer covers the whole specimen by 90 days, increasing its coverage and density with time, and has a Ca:P ratio of approximately 1.6 after 7 days, comparable to that of stoichiometric HA (Ca: P, 1.67). However G-XRD did not detect any crystalline calcium phosphate phases at the surface of the cement up to 90 days (Fig. 9), indicating that the surface layer is amorphous in nature. It is likely given the EDX data and lack of crystalline peaks from the G-XRD that an amorphous calcium phosphate (ACP) is present at the surface of the cement. The nucleation of this layer begins at precise sites on the substrate. Si-OH [38] and COOH [39]

groups have been shown to be effective nucleation sites in the formation of apatite and both are abundant at the surfaces of GICs. Once sufficient Ca is released, the IP of HA increases at the cement-SBF interface, and ionic deposition of a critical nucleus occurs. This nucleus marks the point at which the energy barrier for apatite nucleation has been exceeded, and the nucleus then grows by further ionic deposition from the SBF. The lack of crystallinity of this layer is likely to be due to the inhibitory effects of released zinc ions on the crystallization kinetics of HA [40]. However, the formation of a calcium phosphate is likely to accelerate the integration of this cement with surrounding tissues *in vivo*. These results indicate that this cement is bioactive, and is in direct disagreement with work by Kamitakahara *et al.* [30] who concluded that PAA released from GICs retards the formation of a bioactive layer at the surface of GICs in SBF.

Acknowledgments

The financial assistance of the Materials and Surface Science Institute (University of Limerick) and the Commercialisation Fund, Enterprise Ireland (Proof of Concept Grant # PC/2003/001) are gratefully acknowledged.

References

1. J. INSALL and G. SCUDERI, in "Controversies in Total Knee Arthroplasty" (University Press, Oxford, 2001) p. 163.
2. W. PETTY, *J. Bone and Joint Surgery* **60a** (1978) 492.
3. *Idem.*, *ibid.* **60a** (1978) 752.
4. A. T. BERMAN, J. L. PARMET, S. P. HARDING, C. L. ISRAELITE, K. CHANDRASEKAREN, J. C. HARROW, M. D. SINGER and H. ROSENBERG, *ibid.* **80a** (1998) 389.
5. R. SKRIPITZ and P. ASPENBERG, *Biomaterials* **20** (1999) 351.
6. J. W. NICHOLSON, *ibid.* **19** (1998) 485.
7. A. O. AKINMADE and J. W. NICHOLSON, *J. Mat. Sci. Mat. Med.* **4** (1993) 95.
8. A. D. WILSON, *J. Dent. Res.* **62** (1983) 590.
9. J. W. MCCLEAN, *Br. Dent. J.* **164** (1988) 293.
10. P. V. HATTON and I. M. BROOK, *Biomaterials* **19** (1998) 565.
11. J. W. NICHOLSON and A. D. WILSON, "Acid-Base Cements, Their Biomedical and Industrial Applications" (University Press, Cambridge, 1993).
12. J. W. NICHOLSON, J. H. BRAYBROOK and E. A. WASSON, *J. Biomater. Sci. Polymer Edn.* **2** (1991) 277.
13. J. A. WILLIAMS and R. W. BILLINGTON, *J. Oral Rehabil.* **16** (1989) 475.
14. L. D. QUARLES, G. MURPHY, J. B. VOGLER and M. K. DREZNER, *J. Bone Miner. Res.* **5** (1990) 625.
15. M. C. BLADES, D. P. MOORE and P. A. REVELL, *J. Mat. Sci. Mat. Med.* **9** (1998) 701.
16. I. WAKAYAMA, K. J. SONG, V. R. NERURKAR, S. YOSHIDA and R. M. GARRUTO, *Brain Res.* **748** (1997) 237.
17. S. POLIZZI, E. PIRA, M. FERRARA, B. MASSIMILIANO, A. PAPALEO, R. ALBERA and S. PALMI, *NeuroToxicology.* **23** (2002) 761.
18. C. EXLEY, *J. Inorg. Biochem.* **76** (1999) 133.
19. G. W. GUO and Y. X. LIANG, *Brain Res.* **888** (2001) 221.
20. E. REUSCHE, P. PILZ, G. OBERASCHER, B. LINDNER, R. EGENSEPGER, K. GLOECKNER, E. TRINKA and B. IGLSEDER, *Human Pathology* **32** (2001) 1136.
21. S. G. GRIFFIN and R. G. HILL, *Biomaterials* **20** (1999) 1579.
22. A. ROSENTHAL and S. H. GAROFLAINI, *J. Am. Ceram. Soc.* **70** (1987) 821.
23. E. R. SEGNIT, *ibid.* **37** (1954) 273.
24. M. DARLING and R. G. HILL, *Biomaterials* **15** (1994) 229.
25. M. R. TOWLER, C. M. CROWLEY, D. MURPHY and M. C. O'CALLAGHAN, *J. Mat. Sci. Mat. Med.* **21** (2002) 1123.
26. M. YAMAGUCHI and T. MATSUI, *Peptides* **17** (1996) 1207.
27. J. OVESEN, B. MOLLER-MADSEN, J. S. THOMSEN, G. DANSCHER and L. MOSEKILDE, *Bone* **29** (2001) 565.
28. H. S. NALWA, in "Handbook of Organic-Inorganic Hybrid Materials and Nanocomposites vol. 2, Nanocomposites" (American Scientific Publishers, California, 2003).
29. T. KOKUBO, H. KUSHITANI, S. SAKKA, T. KITSUGI and T. YAMAMURO, *J. Biomed. Mat. Res.* **24** (1990) 721.
30. M. KAMITAKAHARA, M. KAWASHITA, T. KOKUBO and T. NAKAMURA, *Biomaterials* **22** (2001) 3191.
31. A. SULLIVAN and R. G. HILL, *J. Mat. Sci.* **35** (2000) 1125.
32. International standard 9917:1991 (E). Dental Water Based Cements. International Organization for Standardization, Case Postale 56, CH-1211, Geneve, Switzerland.
33. J. A. WILLIAMS, R. W. BILLINGTON and G. J. PEARSON, *Dent. Mater.* **18** (2002) 376.
34. J. A. WILLIAMS, R. W. BILLINGTON and G. J. PEARSON, *Brit. Dent. J.* **172** (1992) 279.
35. M. R. TOWLER, C. C. FRANCE and R. W. BILLINGTON, *J. Dent. Res.* **77/B** (1998) Abs#3117.
36. International standard 5833:1992 (E). Implants for Surgery Acrylic Resin Cements. International Organization for Standardization, Case Postale 56, CH-1211, Geneve, Switzerland.
37. J. W. NICHOLSON, P. J. BROOKMAN, O. M. LACY, G. S. SAYERS and A. D. WILSON, *J. Biomed. Mat. Res.* **22** (1988) 623.
38. P. LI, T. OHTSUKI, T. KOKUBO, K. NAKANISHI, N. SOGA, T. NAKAMURA and T. YAMAMURO, *J. Mat. Sci. Mat. Med.* **4** (1993) 127.
39. M. TANAHASHI and T. MATSUDA, *J. Biomed. Mat. Res.* **34** (1997) 305.
40. N. KANZAKI, K. ONUMA, G. TREBOUX, S. TSUTSUMI and A. ITO, *J. Phys. Chem.* **104** (2000) 4189.

Received 7 April
and accepted 17 December 2004